

# Hepatocellular Carcinoma: Microwave Ablation with Multiple Straight and Loop Antenna Clusters—Pilot Comparison with Pathologic Findings<sup>1</sup>

Nam C. Yu, MD  
 David S. K. Lu, MD  
 Steven S. Raman, MD  
 Damian E. Dupuy, MD  
 Caroline J. Simon, MD  
 Charles Lassman, MD  
 Bassam I. Aswad, MD  
 David Ianniti, MD  
 Ronald W. Busuttil, MD, PhD

The purpose of this study was to evaluate the clinical implementation of triangular and spherical designs for simultaneous multiple-antenna ablation of human hepatocellular carcinoma (HCC) with a recently engineered microwave coagulation system. Institutional review board approval and informed consent were obtained, and the study was compliant with HIPAA requirements. Nine patients (five men, four women; age range, 53–79 years; mean age, 66.2 years) with resectable HCC (diameter, 2.9–6.0 cm; mean, 4.2 cm) underwent intraoperative ultrasonography-guided tumor ablation followed by resection and pathologic examination. Standard single-straight ( $n = 2$ ), triangular triple-straight ( $n = 4$ ), and spherical triple-loop ( $n = 3$ ) antenna configurations produced mean estimated coagulation volumes of 16.7, 51.7, and 54.3 cm<sup>3</sup>, respectively, during a single concurrent 5–10-minute ablation cycle. The triple-loop configuration yielded the most uniformly round ablation shape. Simultaneous activation of multiple straight or loop antennae is a potentially promising technique for rapid and effective treatment of large HCCs.

© RSNA, 2006

<sup>1</sup> From the Departments of Radiological Sciences (N.C.Y., D.S.K.L., S.S.R.), Pathology (C.L.), and Surgery (R.W.B.), David Geffen School of Medicine at UCLA, BR-158 CHS, Box 951721, 10833 Le Conte Ave, Los Angeles, CA 90095-1721; and the Departments of Diagnostic Imaging (D.E.D., C.J.S.), Pathology (B.I.A.), and Surgery (D.I.), Brown Medical School, Providence, RI. Received September 14, 2004; revision requested November 19; revision received March 1, 2005; accepted March 16; final version accepted May 4. Supported by Vivant Medical, Mountain View, Calif. **Address correspondence to** D.S.K.L.

© RSNA, 2006

**H**epatocellular carcinoma (HCC) is one of the most prevalent and fatal of all malignancies worldwide. In particular, its incidence in the United States continues to escalate, correlating with an increase in chronic hepatitis C cirrhosis (1). Given the unresectability of most tumors at the time of diagnosis, local thermoablative techniques have been widely integrated into the therapeutic repertoire. Among these, radiofrequency (RF) ablation remains the most universally adopted, and its use is supported by good safety and efficacy profiles (2–4). Microwave ablation is used as an alternative in some Asian institutions, and the results of several studies have validated similar clinical success (5–7).

RF ablation and microwave ablation share several common advantages and disadvantages. They both allow flexible treatment approaches, including percutaneous, laparoscopic, or open surgical access, with convenient ultrasonographic (US) or computed tomographic (CT) guidance. Furthermore, because local targeting results in the effective sparing of uninvolved liver tissue, treatments are generally well tolerated, even in patients with limited hepatic reserve. Perhaps the most commonly cited drawback is the difficulty in treating large tumors, which are routinely defined as those exceeding 3 cm in diameter. Indeed, with current technology it is challenging to create reproducibly large coagulation volumes. As a result, treatment of large tumors is notoriously cumbersome and time consuming, requiring multiple sequential overlapping ablations to ensure adequate coverage (8,9). Even with such meticulous measures, high recurrence rates remain the rule (10,11).

One proposed solution to this dilemma involves the use of arrays with multiple probes to achieve larger coagulation volumes. The two ablation modalities differ substantially in the basic mechanism of energy deposition. RF ablation uses the flow of current through conducting electrodes within body tissue, while microwave ablation uses an electromagnetic field around an insulated and electrically independent antenna. Consequently, microwave ablation is theoretically more amenable to

the simultaneous use of multiple probes to achieve larger coagulation volumes, whereas similar applications with monopolar RF ablation may be limited by electrical interference between the individual electrodes (12,13).

Previously, a microwave ablation system engineered in the United States was tuned to the dielectric properties of liver tumors (14) for optimized specific absorption rate distribution (15); this system was equipped to activate multiple antennae independently and simultaneously. Previous *in vivo* experiments with triple-antenna ablations in the porcine liver have produced synergistically larger, more uniform lesions (16) and have shown promise for more convenient and effective treatment of large tumors. In addition to triple-antenna ablation, modification of antenna-tip geometry may provide further advantages with regard to lesion size and shape. For example, one commonly used RF device employs curved tines that form an umbrella shape when deployed. A microwave antenna in the shape of a circular loop, which theoretically allows for enhanced tumor targeting and more spherical ablations, has also been designed. Animal experiments have been performed by using prototypes with single or double orthogonal loop configurations (17). We report herein our experience in clinically implementing triangular and spherical designs for simultaneous multiple-antenna ablation of human HCC with a recently engineered microwave coagulation system.

### Materials and Methods

This study was financially supported by Vivant Medical (Mountain View, Calif). Two of the authors (D.S.K.L. and D.E.D.) receive grant support from and are paid consultants of Vivant Medical. All data and information that might have presented a potential conflict of interest for these authors were controlled by those authors who were not affiliated with Vivant Medical.

### Patient Population

Our study was compliant with the Health Insurance Portability and Ac-

countability Act and was approved by the institutional review boards of the respective institutions; informed consent was obtained from all patients. From August 2003 to January 2004, 20 patients with indications for liver tumor resection were prospectively recruited from two academic centers in the United States (Table 1). Nine of 20 patients had HCC and were included in this study. The patient population included five men and four women (mean age, 66.2 years; age range, 53–79 years). All patients had undergone multiphase CT or gadolinium-enhanced magnetic resonance (MR) imaging to delineate the target tumor and to assist in surgical planning. Initial diagnosis of HCC was based on biopsy findings or classic imaging characteristics of tumor hypervascularity, with either elevated  $\alpha$ -fetoprotein levels or growth of a nodule over time. For each patient, only a single HCC lesion was present. All tumors were subcapsular, and three were exophytic.

### Microwave Ablation Device

The ablation system that was used was a VivaWave Microwave Coagulation System (Vivant Medical). Each generator was capable of producing 60 W of power at 915 MHz. Each antenna was connected to a generator by means of a coaxial cable. One of three antenna configurations was employed for each

#### Published online before print

10.1148/radiol.2383041592

**Radiology 2006**; 239:269–275

#### Abbreviations:

HCC = hepatocellular carcinoma  
NADH = nicotinamide adenine dinucleotide, reduced  
RF = radiofrequency

#### Author contributions:

Guarantor of integrity of entire study, N.C.Y.; study concepts/study design or data acquisition or data analysis/interpretation, all authors; manuscript drafting or manuscript revision for important intellectual content, all authors; manuscript final version approval, all authors; literature research, N.C.Y., D.E.D., C.J.S., D.I.; clinical studies, D.E.D., C.J.S., B.I.A., D.I., R.W.B.; statistical analysis, N.C.Y., D.I.; and manuscript editing, N.C.Y., D.S.K.L., D.E.D., C.J.S., C.L., D.I.

See Materials and Methods for pertinent disclosures.

ablation: (a) a standard single-straight antenna configuration ( $n = 2$ ), (b) a triangular triple-straight antennae configuration ( $n = 4$ ), and (c) a spherical triple-loop antenna configuration that formed a cage ( $n = 3$ ). The attending interventional radiologist selected the configuration and target location of the antennae for each case, with selection based on tumor size, tumor location and accessibility, and expected resection plane. The goal was to confine coagulation within the resected specimen and to preserve a portion of viable tumor for pathologic analysis as a control.

For the single-antenna ablations, only one generator was employed; for the triangular and spherical ablations, each antenna component was connected to one of three independent generators. The straight antenna had a 13-gauge diameter, a 15-cm length, and a 3.6-cm antenna tip. The triangular array was formed with a rigid spacer that separated the three individual straight antennae by 1.5 cm ( $n = 1$ ) or 2.0 cm ( $n = 3$ ). The spherical array consisted of three 13-gauge shafts, each with a wirelike antenna tip that was deployed into a circular loop after positioning in the target tissue. The three antenna loops, each 3 cm in diameter, approximated a spherical cage to allow ablation of the circumscribed volume, as well as of a margin of tissue outside the 3-cm sphere.

#### Microwave Ablation Protocol: Ablation and Resection

All intraoperative US and microwave ablations were performed by one of two attending interventional radiologists (D.S.K.L. and D.E.D., both with 11 years of experience in ablation). A general anesthetic was administered, and exposure of the liver was performed in standard fashion by the hepatobiliary surgical team. The index tumor that was previously seen at CT or MR imaging was identified by means of US, and the rest of the liver was scanned with US to ensure the absence of other suspicious nodules. The antenna was then targeted to the tumor by using continuous US guidance. For the spherical configuration, insertion of the antenna

was followed by cautery-assisted deployment of the three loops, with the antenna cables connected to a surgical cautery generator. Cautery allowed smooth and unhindered deployment of the loops by allowing the antenna to cut through the liver tissue. The properly deployed loops, which formed a cage structure around the target lesion, could be confirmed with US.

For all straight antennae in either single or triangular configuration, ablation was performed at 45 W for 6–10 minutes, depending on the size of the tumor and on the location of the planned resection plane. The loop antennae were powered at 60 W for 5 minutes. For both the triangular and spherical configurations, all three generators were activated simultaneously to achieve a synchronous ablation. Only a single ablation cycle was applied in all cases. Continuous US monitoring was

used to track the progress of ablation, and the extension of the coagulation front could be approximated on the basis of the transient hyperechoic zone. After completion of the cycle, the antennae were removed, and tumor resection commenced. For the spherical configuration, the loop antennae were first retracted back into the shaft prior to removal from the liver.

No immediate complications secondary to microwave ablation were noted. Postoperative complications, including renal failure, perihepatic abscess, and liver decompensation, were noted in four patients.

#### Pathologic Analysis

Specimens containing the entire tumor and ablation lesions were immediately processed after resection by one of two liver pathologists (C.L. and B.I.A., with 8 and 10 years of experience, respec-

**Table 1**

#### Patient and Tumor Characteristics

Patient No./ Sex/Age (y)	Liver Disease	Tumor Size* (cm)	Histologic Grade <sup>†</sup>	Location (Couinaud Segment)	Antenna Configuration
1/M/72	Hepatitis B	2.9	2	VII	Single straight
2/F/79	Hepatitis C	5.0	2	IVb	Triple straight
3/F/53	Hepatitis C	5.3	2	I	Triple straight
4/M/65	Hepatitis C	3.7	2	II	Single straight
5/M/64	Hepatitis B	3.4	2	VIII	Triple loop
6/F/63	Hepatitis C	4.0	2	VII and VIII	Triple loop
7/M/57	Hepatitis C	2.0	2	VII	Triple straight
8/M/77	Cryptogenic	5.7	2	VI and VII	Triple straight
9/F/45	Hepatitis C	6.0	3	IV	Triple loop

\* Diameter in long axis.

<sup>†</sup> Histologic grade was determined on a scale of 1–4 on the basis of the Edmondson-Steiner grading system. Tumor was well differentiated in patients 1–8 and moderately differentiated in patient 9.

**Table 2**

#### Size Characteristics of Ablated Lesions

Antenna Configuration	Short-Axis Diameter (cm)	Long-Axis Diameter (cm)	Estimated Volume (cm <sup>3</sup> )
Single straight ( $n = 2$ )	2.5–2.7 (2.6)	3.8–4.0 (3.9)	12.4–20.9 (16.7)
Triple straight ( $n = 4$ )	3.0–4.5 (3.7)	5.0–6.3 (5.6)	45.7–58.7 (51.7)
Triple loop ( $n = 3$ )	3.4–4.1 (3.7)	5.0–6.4 (5.7)	47.1–58.9 (54.3)

Note.—Data are the range, with mean values in parentheses.

tively). In all cases, the diagnosis of HCC was confirmed by means of histologic criteria. The specimens were sliced into sections that were roughly 0.5 cm thick for pathologic analysis and digital photography at gross examination. Representative regions of interest, which generally included coagulated and viable tumor, coagulated and viable

liver, and equivocal areas at the transition zones, were then processed by means of frozen sectioning. The rem-

nant viable tumor (present in six of nine specimens) served as a control to allow comparative characterization of histologic changes owing to coagulation within the ablated tumor.

The sections were subjected to standard hematoxylin-eosin staining and vital histochemical staining for the mitochondrial enzyme nicotinamide adenine dinucleotide, reduced (NADH) diaphorase. The histochemical sections were then superimposed over the hematoxylin-eosin sections and digital photographs obtained at gross examination to determine tissue viability in the regions of interest. The resection margins were also scrutinized for tumor according to a standard clinical protocol. Approximate volumes ( $V$ ) for the tumor and coagulation zone were calculated with the ellipsoid equation  $V = 1/6 \cdot \pi \cdot x \cdot y \cdot z$ , where  $x$ ,  $y$ , and  $z$  represent the diameters in the three orthogonal axes.

### Data Analysis

Descriptive data analyses (mean and range) were performed by using a commercially available software program (InStat v3.05; GraphPad, San Diego, Calif).

### Results

#### Ablation Lesion Characteristics

Maximal ablation diameters for the two single-straight antenna ablations were 3.8 and 4.0 cm, with volumes of 12.4 and 20.9  $\text{cm}^3$ , respectively. Triangular clusters ( $n = 4$ ) resulted in a mean diameter of 5.6 cm (range, 5.0–6.3 cm) and a mean volume of 51.7  $\text{cm}^3$  (range, 45.7–58.7  $\text{cm}^3$ ). For the three ablations that were performed with the spherical array, the diameters were 5.6, 6.4, and 5.0 cm, with volumes of 56.9, 58.9, and 47.1  $\text{cm}^3$ , respectively; the smallest volume was obtained in a scirrhous-type HCC. Short- and long-axis diameters and volume data are provided in Table 2. Of note, all coagulated lesions demonstrated some degree of asymmetry, as indicated by the dissimilar diameters in the short and long axes. The single-straight antenna configuration appeared to produce ablations that were slightly

**Figure 1**

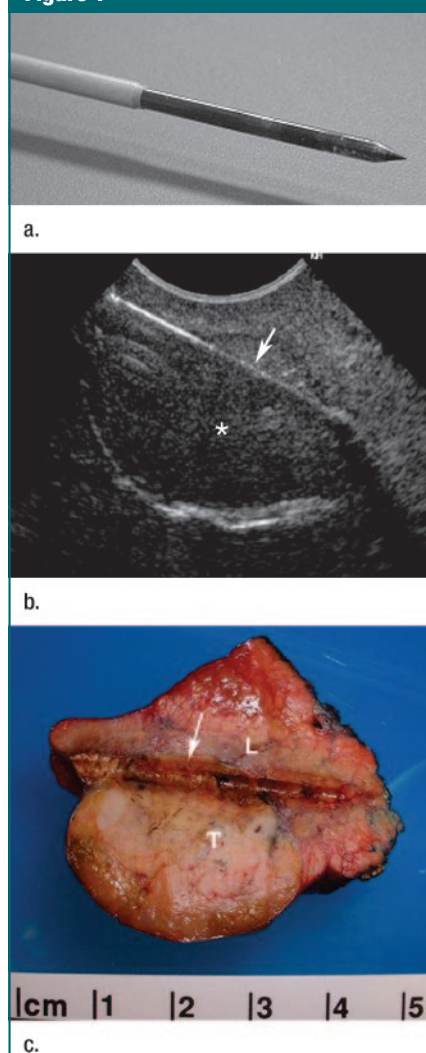


**Figure 1:** (a) Single-straight probe composed of standard rigid shaft with 3.6-cm antenna tip. (b) US image shows antenna (arrow) of single-straight probe inserted into the base of an exophytic HCC (\*). (c) Gross pathologic examination of transected mass reveals shaft recess (arrow) surrounded by tan areas of coagulated tumor (T) and liver (L). Note that the coagulation front has progressed farther in the tumor than in the liver.

**Figure 2**

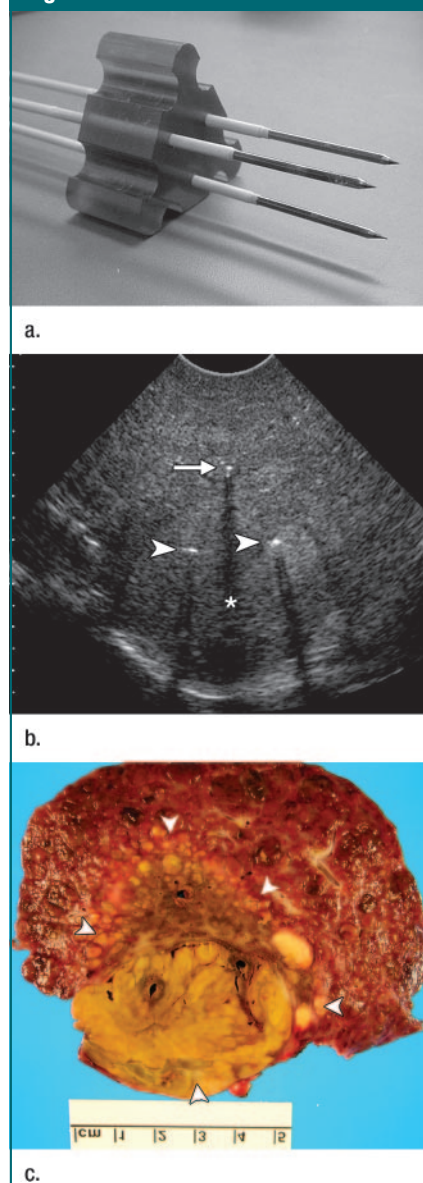


**Figure 2:** (a) Triple-straight probe composed of three individual antennae held in a triangular array with a 2.0-cm rigid spacer. (b) US image shows two antennae (arrowheads) targeted to positions at the base of an exophytic tumor (\*) and one antenna (arrow) in the surrounding liver. (c) Resected specimen shows coagulation borders (arrowheads), which suggest a slight loss of convexity that was more pronounced in the cirrhotic liver tissue than in the tumor.

Figure 3

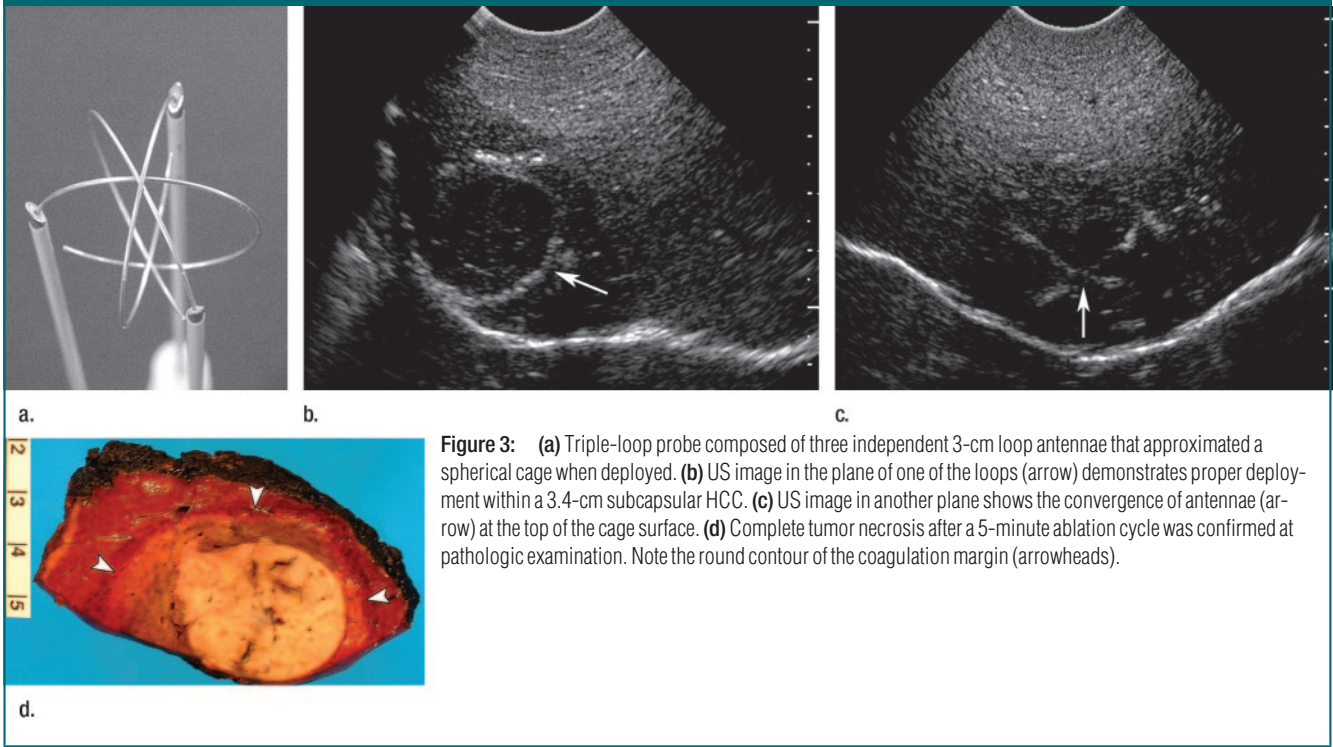


**Figure 3:** (a) Triple-loop probe composed of three independent 3-cm loop antennae that approximated a spherical cage when deployed. (b) US image in the plane of one of the loops (arrow) demonstrates proper deployment within a 3.4-cm subcapsular HCC. (c) US image in another plane shows the convergence of antennae (arrow) at the top of the cage surface. (d) Complete tumor necrosis after a 5-minute ablation cycle was confirmed at pathologic examination. Note the round contour of the coagulation margin (arrowheads).

ellipsoid such that the long diameter of the coagulated zone corresponded to the axis of the antenna shaft (Fig 1). For the triangular (Fig 2) and spherical (Fig 3) configurations, which produced larger lesions, the asymmetry was imposed by the liver edge, which necessarily demarcated the lesion border (Fig 3c).

In all triangular ablations, the lesion components that were created by each antenna had completely fused to form one large, continuous volume. Nevertheless, lesion shapes revealed that the cross sections perpendicular to the antenna shafts were not strictly circular and showed a slightly triangular contour (Fig 2c). This deformation, however, was limited enough that concave clefts along the coagulation border could not be seen at gross examination. During the spherical ablations, tissue heating that progressed from the exterior had fully converged at the center such that all enclosed tissue, along with 0.5–1.0 cm of tissue exterior to the cage surface, appeared at gross examination to have undergone uniform coagulation.

### Microscopic Examination

While gross examination was adequate to determine the general shape and approximate dimensions of the ablation zones, histochemical staining was employed to rigorously analyze the extent of cell death. Features seen with hematoxylin-eosin staining, however, were often equivocal. Thus, viable and nonviable tissue could not be distinguished reliably. In most areas, coagulation was more apparent in the gross specimen than in the sections prepared with hematoxylin-eosin staining for which cell death was sometimes marked only by a subtle loss of nuclear chromatin detail.

On the other hand, histochemical staining for the mitochondrial enzyme NADH diaphorase definitively reflected cellular viability because of the unambiguous binary staining characteristics that were demonstrated—that is, positive staining indicated viability and the absence of staining indicated cell death. For all specimens, uniform necrosis within ablated regions at gross examination could be confirmed with histochemical staining for NADH diaphorase. At

the borders, gross examination typically showed an indistinct zone of transition, approximately 0.5 cm wide, between clearly coagulated and clearly viable tissue. Histochemical staining for NADH diaphorase consistently revealed uniform cell death extending through this transition zone, with a sharp border demarcating viable from ablated regions (Fig 4). This finding could be confirmed by directly comparing histochemical-stained sections with the corresponding gross specimens and hematoxylin-eosin-stained sections.

### Discussion

While RF and microwave ablation devices employ a common agent for tumor destruction—namely, heat—they differ considerably in the basic mechanism underlying energy deposition. Heat produced with microwave energy, unlike that produced with RF energy, does not depend on the passage of electrical current through the tissue, thereby allowing simultaneous activation with multiple antennae without the electrical in-

interference encountered in current RF systems (12). Multipolar RF technology (18) or the rapid switching of power between multiple electrodes (19) may prove useful but currently remains relatively untested in the clinical setting. While some authors have studied the use of multiple microwave antennae (20,21), the antennae were activated sequentially rather than simultaneously. The current study describes a prototype microwave ablation system that was adapted for the simultaneous activation of recently designed, multiple-antenna clusters to achieve efficient production of large and controlled coagulation volumes.

The results of initial experiments by other investigators (16) who used por-

pine liver proved promising. Coagulation volumes obtained with simultaneously powered multiple straight antennae significantly exceeded the additive volumes obtained with the same number of ablations performed sequentially. Furthermore, such synergistically larger volumes could be obtained in the time that is required for a single ablation cycle by virtue of the simultaneous activation of all antennae. We used this device for human HCC in the setting of preliminary clinical testing. With the triangular triple-straight antenna configuration, large lesions (ie, those with a volume of approximately 50 cm<sup>3</sup>) could be created in 10 minutes or less, which is comparable with the results reported in the porcine study. In our study, however, the increase in size for triple-straight antenna ablations compared with single-antenna ablations was not as dramatic as that seen in the porcine liver, which demonstrated a sixfold increase in ablation size. This correlated with the observation that our single-antenna ablations produced larger lesions relative to the porcine counterpart.

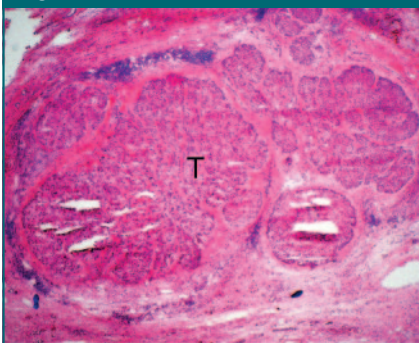
Two effects may be responsible. First, we theorize that larger volumes are obtained in HCC than in liver parenchyma because of the differences in tissue characteristics. This is consistent with the findings of previous RF ablation studies, which demonstrated that significantly larger ablations were achieved in livers with large tumors than in those with small or no tumors (11,22); findings in these studies were presumably secondary to differing thermal and perfusion properties. For our microwave system, the antennae were optimized for the dielectric properties of liver tumors (14), which may have accentuated the disparity. During the multiple-antenna ablations, ablation volume was larger and more likely to extrude into the surrounding liver, where a greater barrier to lesion growth was encountered. Second, and perhaps more important, the larger multiple-antenna lesions were often confined by the liver edge, given that the subcapsularity of the tumor necessarily limited the ablation size to the liver edge. These factors

account for the larger coagulation volume achieved in HCC compared with porcine liver by using single-antenna ablation. Compared with multiple-antenna ablation, which produced coagulation zones extending well beyond the tumor to the liver edge or parenchyma, single-antenna ablation produced lesions that were predominantly enclosed within tumor, resulting in roughly linear (rather than synergistically exponential) volume increases for the multiple-antenna ablations.

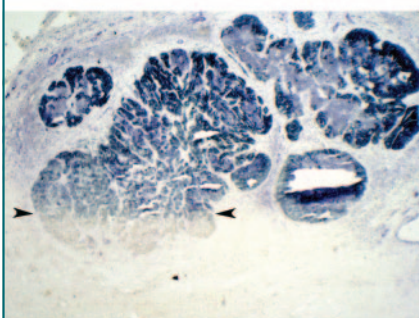
One potential disadvantage of the triangular configuration was that it tended to result in a nonspherical volume, as may be expected from the triangular arrangement of the three antennae. In the porcine study, antenna separation beyond 1.7 cm was associated with ablation contours that were significantly less round. When the 2.0-cm spacing was used in our study, a loss of border convexity was noted, particularly in the cirrhotic liver, where ablation zones from the individual antennae demonstrated less overlap. In all cases, however, the zones had adequately fused such that clefts of spared tissue could not be seen between the antennae.

Given its symmetric design, the spherical triple-loop configuration may overcome this limitation by producing a more controlled and rounder ablation zone. If the spherical cage is deployed to encompass the target nodule, coagulation can proceed "from the outside in." As long as proper deployment can be confirmed, the enclosed tissue, along with the tissue margin exterior to the cage, can be ablated with greater accuracy. Results from a previous study that used single- and double-loop designs in the porcine liver showed the potential merits of this approach (17). Nonspherical geometry and spared central tissue, however, were noted in some cases. The use of three loops rather than two provides a more optimal cage geometry to facilitate the creation of spherical lesions, and although the liver edge tended to impose an overall asymmetry in the lesion, the ablation borders within the tissue exhibited adequate uniform roundness. Furthermore, the additional loop presumably allows for

**Figure 4**



**a.**



**b.**

**Figure 4:** (a) Histologic section obtained at coagulation margin shows satellite tumor nodule cluster (T) in the background of cirrhotic liver. (Hematoxylin-eosin stain; original magnification,  $\times 20$ .) (b) Histologic section in the same field allows clear differentiation of viable (upper) and ablated (lower) zones, with a sharp line of demarcation (arrowheads) traversing the nodule. (Histochemical stain; original magnification,  $\times 20$ .)

the potential of synergism to produce even higher temperatures around the cage, thereby ensuring complete necrosis within and exterior to the cage. Indeed, uniform coagulation inside the 3-cm cage without any central sparing was seen at gross examination and was confirmed with histochemical staining for NADH diaphorase.

A major disadvantage of simultaneous multiple-antenna microwave ablation is the greater difficulty in placing all antennae with respect to the index tumor. Even with real-time US, it may be cumbersome to visualize all components for precise positioning. This is especially problematic for the loop configuration because all three shafts must be inserted simultaneously, which requires greater operator skill in US guidance and mental reconstruction of three-dimensional structures. Thus, an initial learning-curve effect may be seen. We do not, however, expect this challenge to pose a major barrier for experienced interventionists. A related disadvantage of multiple-antenna ablation is that it cannot be easily implemented for the percutaneous approach, which has a more limited window of access.

This study was limited to a few cases for each antenna configuration. Thus, our findings provided useful observations but no conclusive characterization of the ablative lesions. For example, the data are not sufficient to enable reliable prediction of absolute ablation dimensions for a given applicator. Further clinical experience that accounts for several potential variables, such as tumor type, liver perfusion, generator power, and cycle time, will be required to characterize more precisely the ablation zones in various situations. Another limitation of the study was that the synergistic volume effect of simultaneous ablation was not proved by using a control group treated with sequential activation. Given the limited sample size and subcapsular or exophytic location of the tumors (as discussed previously), such comparisons were not feasible. Hence, the porcine model is more useful for such scientific investigations (16), whereas we were limited to descriptive reporting.

In conclusion, this pilot study provides encouraging results for simultaneous multiple-antenna microwave ablation of HCC. Relatively large coagulation volumes can be achieved in short procedure times with these antenna arrays, which may enable more effective treatment of large tumors with lower complication rates. In particular, the spherical triple-loop configuration appears promising for the creation of sizable, controlled, and rounder lesions. Treatment studies are warranted and are currently underway to test clinical efficacy.

### References

1. El-Serag HB, Mason AC. Rising incidence of hepatocellular carcinoma in the United States. *N Engl J Med* 1999;340:745-750.
2. Lau WY, Leung TW, Yu SC, Ho SK. Percutaneous local ablative therapy for hepatocellular carcinoma. *Ann Surg* 2003;237:171-179.
3. Curley SA, Izzo F, Ellis LM, Nicolas Vauthey J, Vallone P. Radiofrequency ablation of hepatocellular cancer in 110 patients with cirrhosis. *Ann Surg* 2000;232:381-391.
4. Lencioni R, Cioni D, Bartolozzi C. Percutaneous radiofrequency thermal ablation of liver malignancies: techniques, indications, imaging findings, and clinical results. *Abdom Imaging* 2001;26:345-360.
5. Xu HX, Xie XY, Lu MD, et al. Ultrasound-guided percutaneous thermal ablation of hepatocellular carcinoma using microwave and radiofrequency ablation. *Clin Radiol* 2004;59:53-61.
6. Shibata T, Iimuro Y, Yamamoto Y, et al. Small hepatocellular carcinoma: comparison of radio-frequency ablation and percutaneous microwave coagulation therapy. *Radiology* 2002;223:331-337.
7. Dong B, Liang P, Yu X, et al. Percutaneous sonographically guided microwave coagulation therapy for hepatocellular carcinoma: results in 234 patients. *AJR Am J Roentgenol* 2003;180:1547-1555.
8. Dodd GD, Frank MS, Aribandi M, et al. Radiofrequency thermal ablation: computer analysis of the size of the thermal injury created by overlapping ablations. *AJR Am J Roentgenol* 2001;177:777-782.
9. Chen MH, Yang W, Yan K, et al. Large liver tumors: protocol for radiofrequency ablation and its clinical application in 110 patients—mathematic model, overlapping mode, and electrode placement process. *Radiology* 2004;232:260-271.
10. Livraghi T, Goldberg SN, Lazzaroni S, et al. Hepatocellular carcinoma: radiofrequency ablation of medium and large lesions. *Radiology* 2000;214:761-768.
11. Kuvshinov BW, Ota DM. Radiofrequency ablation of liver tumors: influence of technique and tumor size. *Surgery* 2002;132:605-611.
12. Goldberg SN, Gazelle GS, Dawson SL, Rittman WJ, Mueller PR, Rosenthal DI. Tissue ablation with radiofrequency using multiprobe arrays. *Acad Radiol* 1995;2:670-674.
13. Goldberg SN, Solbiati L, Hahn PF, et al. Large-volume tissue ablation with radiofrequency by using a clustered, internally cooled electrode technique: laboratory and clinical experience in liver metastases. *Radiology* 1998;209:371-379.
14. Stauffer PR, Rossetto F, Prakash M, Neuman DG, Lee T. Phantom and animal tissues for modeling the electrical properties of human liver. *Int J Hyperthermia* 2003;19:89-101.
15. Lin JC, Wang YJ. The cap-choke catheter antenna for microwave ablation treatment. *IEEE Trans Biomed Eng* 1996;43:657-660.
16. Wright AS, Lee FT, Mahvi DM. Hepatic microwave ablation with multiple antennae results in synergistically larger zones of coagulation and necrosis. *Ann Surg Oncol* 2003;10:275-283.
17. Shock SA, Meredith K, Warner TF, et al. Microwave ablation with loop antenna: in vivo porcine liver model. *Radiology* 2004;231:143-149.
18. Tacke J, Mahnken A, Roggan A, Gunther RW. Multipolar radiofrequency ablation: first clinical results. *Rofo* 2004;176:324-329.
19. Lee FT Jr, Haemmerich D, Wright AS, Mahvi DM, Sampson LA, Webster JG. Multiple probe radiofrequency ablation: pilot study in an animal model. *J Vasc Interv Radiol* 2003;14:1437-1442.
20. Sato M, Watanabe Y, Kashu Y, Nakata T, Hamada Y, Kawachi K. Sequential percutaneous microwave coagulation therapy for liver tumor. *Am J Surg* 1998;175:322-324.
21. Lu MD, Chen JW, Xie XY, et al. Hepatocellular carcinoma: US-guided percutaneous microwave coagulation therapy. *Radiology* 2001;221:167-172.
22. Montgomery RS, Rahal A, Dodd GD III, Leyendecker JR, Hubbard LG. Radiofrequency ablation of hepatic tumors: variability of lesion size using a single ablation device. *AJR Am J Roentgenol* 2004;182:657-661.